2

SIGNAL PROCESSING

2.0 INTRODUCTION

All of the biomechanical variables are time-varying, and it doesn't matter whether the measure is kinematic, kinetic, or EMG; it must be processed like any other signal. Some of these variables are directly measured: acceleration and force signals from transducers or EMG from bioamplifiers. Others are a product of our analyses: moments-of-force, joint reaction forces, mechanical energy and power. All can benefit from further signal processing to extract cleaner or averaged waveforms, correlated to find similarities or differences or even transformed into the frequency domain.

This chapter will summarize the analysis techniques associated with auto- and cross-correlations, frequency (Fourier) analysis and its applications correct data record length and sampling frequency. The theory of digital filtering is presented here; however, the specific applications of digital filtering of kinematics appears in Chapter 3 and analog filtering of EMG in Chapter 10. The applications of ensemble averaging of variables associated with repetitive movements are also presented.

2.1 AUTO- AND CROSS-CORRELATION ANALYSES

Autocorrelation analyzes how well a signal is correlated with itself, between the present point in time and past and future points in time. Cross-correlation

 ISBN: 978-0-470-39818-0

analyses evaluate how well a given signal is correlated with another signal over past, present, and future points in time. We are familiar in statistics with the Pearson product moment correlation. It is a measure of relationship between two variables and allows us to determine whether a variable x increases or decreases as the variable y increases. The strength and polarity of this relationship is given by the correlation coefficient: the higher the value the stronger the relationship, while the sign indicates if variables x and y are increasing and decreasing together (positive correlation) or if one is increasing while the other is decreasing (negative correlation). The correlation coefficient is a normalized dimensionless number varying from -1 to $+1$.

2.1.1 Similarity to the Pearson Correlation

Consider the formula for the Pearson product moment correlation coefficient relating two variables, x and y:

$$r = \frac{\frac{1}{N}\sum_{i=1}^{N}(x_i - \overline{x})(y_i - \overline{y})}{s_x s_y} \tag{2.1}$$

where: x_i and y_i are the ith samples of x and y, $\overline{x}$ and $\overline{y}$ are the means of x and y, and s_x and s_y are the standard deviations of x and y.

The numerator of the formula is the sum of the product of the two variables after the mean value of each variable has been subtracted. It is easy to appreciate that if x and y are random and unrelated then $(x_i - \overline{x})$ and $(y_i - \overline{y})$ will be scattered in the x-y plane about zero (see Figure 2.1). These products

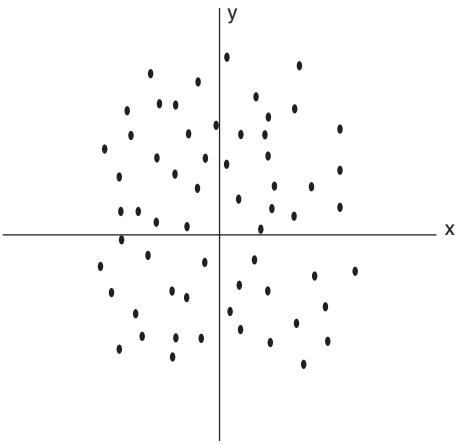

Figure 2.1 Scatter diagram of variable x against variable y showing no relationship between the variables.

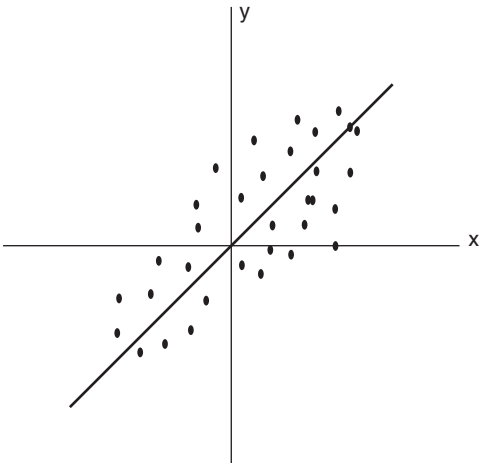

Figure 2.2 Scatter diagram showing a positive correlation between variable x and variable y.

will be $+ve$ in quadrants 1 and 3 and $-ve$ in quadrants 2 and 4, and provided there are enough points their sum, r, will tend towards zero, indicating no relationship between the two variables.

Now if the variables are related and tend to increase and decrease together $(x_i - \overline{x})$ and $(y_i - \overline{y})$ will fall along a line with a positive slope in the x-y plane (see Figure 2.2). When we sum the products in Equation (2.1), we will get a finite $+ve$ sum, and when this sum is divided by N, we remove the influence of the number of data points. This product will have the units of the product of the two variables, and its magnitude will also be scaled by those units. To remove those two factors, we divide by $s_x s_y$, which normalizes the correlation coefficient so that it is dimensionless and lies between -1 and $+1$.

There is an estimation error in the correlation coefficient if we have a finite number of data points, therefore, the level of significance will increase or decrease with the number of data points. Any standard statistics textbook includes a table of significance for the coefficient r, reflecting the error in estimation.

2.1.2 Formulae for Auto- and Cross-Correlation Coefficients

The auto- and cross-correlation coefficient is simply the Pearson product moment correlation calculated on two time series of data rather than on individual measures of data. Autocorrelation, as the name suggests, involves correlating a time series with itself. Cross-correlation, on the other hand, correlates two independent time series. The major difference is that a correlation of time series data does not yield a single correlation coefficient but rather a whole series of correlation values. This series of values is achieved by

shifting one of the series forward and backward in time, the value of this shifting will be evident later. The magnitude ($+ve$ or $-ve$) of this shifting is decided by the user and the time series of correlations is a function of the phase shift, τ. The formula for the autocorrelation of $x(t)$ is $R_{xx}(\tau)$:

$$R_{xx}(\tau) = \frac{\frac{1}{T}\int_0^T x(t)x(t+\tau)dt}{R_{xx}(0)} \tag{2.2}$$

Where: x(t) has zero mean.

The formula for the cross-correlation of $x(t)$ and $y(t)$ is $R_{xy}(\tau)$:

$$R_{xy}(\tau) = \frac{\frac{1}{T}\int_0^T x(t)y(t+\tau)dt}{\sqrt{R_{xx}(0)R_{yy}(0)}} \tag{2.3}$$

where: $x(t)$ and $y(t)$ have zero means.

It is easy to see the similarities between these formulae and the formula for the Pearson product moment coefficient. The summation sign is replaced by the integral sign, and to get the mean we now divide by T rather than N. The denominator in these two equations, as in the Pearson equation, normalizes the correlation to be dimensionless from -1 to $+1$. Also the two time series must have a zero mean, as was the case in the Pearson formula, when the means of x and y were subtracted. Note that the Pearson correlation is a *single* coefficient, while these auto- and cross-correlations are a series of correlation scores over time at each value of τ.

2.1.3 Four Properties of the Autocorrelation Function

Property #1. The maximum value of $R_{xx}(\tau)$ is $R_{xx}(0)$ which, in effect, is the mean square of $x(t)$. For all values of the phase shift, τ, either $+ve$ or $-ve$ $R_{xx}(\tau)$ is less than $R_{xx}(0)$, which can be seen from the following proof.

From basic mathematics we know:

$$\int_0^T (x(t) - x(t-\tau))^2 dt \geq 0$$

Expanding, we get:

$$\int_0^T (x(t)^2 + x(t-\tau)^2 - 2x(t)x(t-\tau))dt \geq 0$$

$$\int_0^T x(t)^2 dt + \int_0^T x(t-\tau)^2 dt - 2\int_0^T x(t)x(t-\tau)dt \geq 0$$

For these integrations, τ is constant; thus, the second term is equal to the first term, and the denominator for the autocorrelation is the same for all terms and is not shown. Thus:

$$R_{xx}(0) + R_{xx}(0) - 2\,R_{xx}(\tau) \geq 0$$
$$R_{xx}(0) - R_{xx}(\tau) \geq 0 \tag{2.4}$$

Property #2. An autocorrelation function is an even function, which means that the function for a $-ve$ phase shift is a mirror image of the function for a $+ve$ phase shift. This can be easily derived as follows; for simplicity, we will only derive the numerator of the equation:

$$R_{xx}(\tau) = \frac{1}{T}\int_0^T x(t)x(t+\tau)dt$$

Substituting $t = (t' - \tau)$ and taking the derivative, we have $dt = dt'$:

$$R_{xx}(\tau) = \frac{1}{T}\int_0^T x(t'-\tau)x(t')dt' = R_{xx}(-\tau) \tag{2.5}$$

Therefore, we have to calculate only the function for $+ve$ phase shifts because the function is a mirror image for $-ve$ phase shifts.

Property #3. The autocorrelation function for a periodic signal is also periodic, but the phase of the function is lost. Consider the autocorrelation of a sine wave; again we derive only the numerator of the equation.

$$x(t) = E\sin(\omega t)$$
$$R_{xx}(\tau) = \frac{1}{T}\int_0^T E\sin(\omega t)E\sin(\omega(t-\tau))dt$$

Using the common trig identity: $\sin(a)\sin(b) = {}^1\!/_2(\cos(a-b) - \cos(a+b))$, we get:

$$R_{xx}(\tau) = \frac{E^2}{2T}\left[t\cos(\omega t) - \frac{1}{2\omega}\sin(2\omega t + \omega\tau)\right]_0^T$$

$$R_{xx}(\tau) = \frac{E^2}{2T}\left[(T\cos(\omega t) - 0) - \frac{1}{2\omega}(\sin(2\omega T + \omega\tau) - \sin(\omega t))\right]$$

Since T is one period of $\sin(\omega t), \therefore \sin(2\omega T + \omega\tau) - \sin(\omega\tau) = 0$ for all τ.

$$\therefore R_{xx}(\tau) = \frac{E^2}{2}\cos(\omega\tau) \tag{2.6}$$

Similarly if $x(t) = E\cos(\omega t)$ also $R_{xx}(\tau) = \frac{E^2}{2}\cos(\omega\tau)$

Note that Equation (2.6) is an even function as predicted by property #2; a plot of this $R_{xx}(\tau)$ after normalization is presented in Figure 2.3.

This property is useful in detecting the presence of periodic signals buried in white noise. White noise is defined as a signal made up of a series of random points, where there is zero correlation between the signal at any point with the signal at any point ahead of or behind it in time. Therefore, at any $\tau \neq 0$ $R_{xx}(\tau) = 0$ and at $\tau = 0$ $R_{xx}(\tau) = 1$. Thus, the autocorrelation of white noise is an impulse, as shown in Figure 2.4.

If we have a signal, $s(t)$, with added noise, $n(t)$, we can express $x(t) = s(t) + n(t)$, and substituting in the numerator of Equation (2.2) we get:

$$\begin{aligned} R_{xx}(\tau) &= \int_0^T (s(t) + n(t))\,(s(t+\tau) + n(t+\tau))\,dt \\ &= \int_0^T s(t)s(t+\tau)dt + \int_0^T n(t)s(t+\tau)dt \\ &\quad + \int_0^T s(t)n(t+\tau)dt + \int_0^T n(t)n(t+\tau)dt \end{aligned}$$

Since the signal and noise are uncorrelated, the 2nd and 3rd terms will $= 0$.

$$\therefore R_{xx}(\tau) = R_{ss}(\tau) + R_{nn}(\tau) \tag{2.7}$$

Property #4. As seen in property #3 the frequency content of $x(t)$ is present in $R_{xx}(\tau)$. The power spectral density function is the Fourier transform of $R_{xx}(\tau)$; more will be said about this in the next section on frequency analysis. However, it is sometimes valuable to use the autocorrelation function to identify any periodicity present in $x(t)$ or to identify the presence of an interfering signal (e.g., hum) in our biological signal. Even if there were no periodicity in $x(t)$, the duration of $R_{xx}(\tau)$ would give an indication of the frequency spectra of $x(t)$; lower frequencies result in $R_{xx}(\tau)$ remaining above zero for longer phase shifts, while high frequencies tend to zero for small phase shifts.

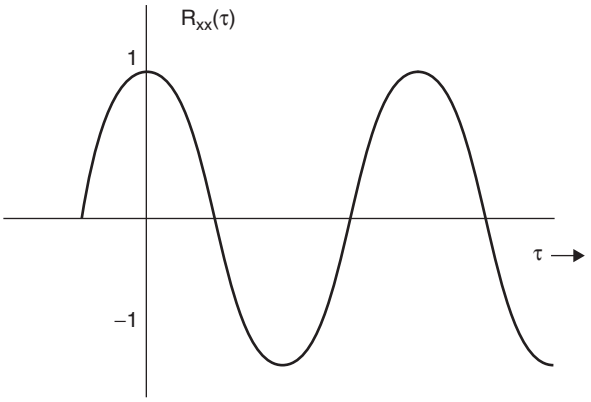

Figure 2.3 Autocorrelation of a sine or cosine signal. Note that this is an even function and the repetitive nature of $R_{xx}(\tau)$ at the frequency of the sine and cosine wave.

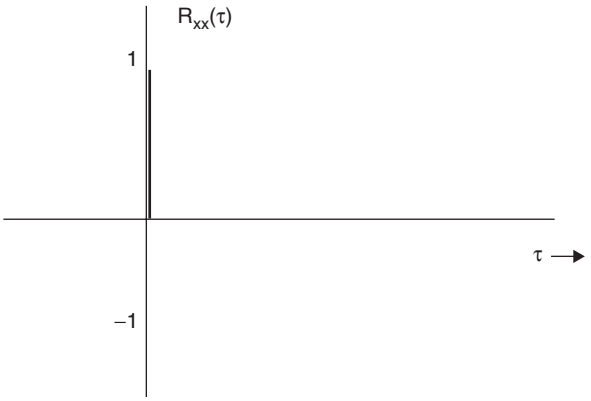

Figure 2.4 Autocorrelation of white noise. Note that $R_{xx}(\tau) = 0$ at all $\tau \neq 0$, indicating that each data point has 0 correlation with all other data points ahead and behind it in time.

2.1.4 Three Properties of the Cross-Correlation Function

Property #1. The cross-correlation of $x(t)$ and $y(t)$ is not an even function. Because the two signals are completely different, the phase shifting in the $+ve$ direction will not result in the same "cross products" as shifting in the $-$ve direction. Thus, $R_{xy}(\tau) \neq R_{xy}(-\tau)$.

Property #2. The maximum value of $R_{xy}(\tau)$ is not necessarily at $\tau = 0$. The maximum $+ve$ or negative peak of $R_{xy}(\tau)$ will occur when the two signals are most in phase or most out of phase. For example, if $x(t)$ is a sine wave and $y(t)$ is a cosine wave of the same frequency at $\tau = 0$, the signals are 90° out of phase with each other, and the cross products over one

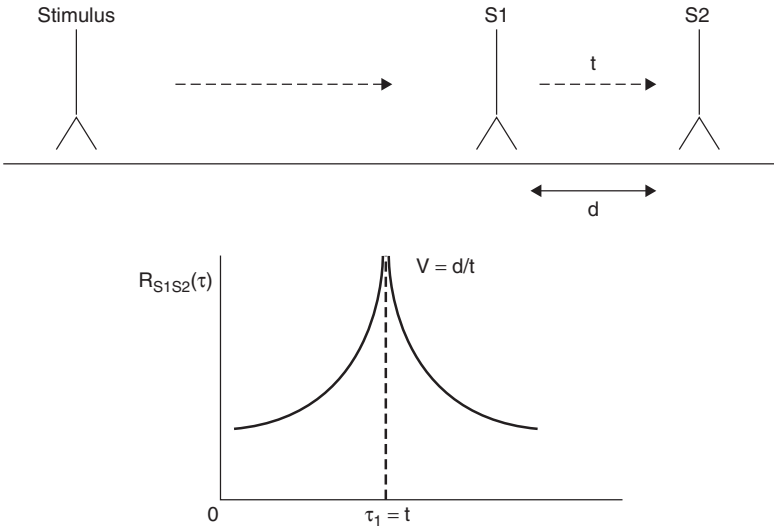

Figure 2.5 Cross-correlation of a neural or muscular signal recorded at two sites, S1 and S2, separated by a distance, d. $R_{xy}(\tau)$ reaches a peak when S2 record is shifted $\tau_1 = t$ sec. Thus, the velocity of the transmission $V = d/t$.

cycle will sum to zero. However, shifting the cosine wave forward 90° will bring the two signals into phase such that all the cross products are $+ve$ and $R_{xy}(\tau) = 1$. Shifting the cosine wave backward 90° will bring the two signals 180° out of phase so that all the "cross products" are −ve and $R_{xy}(\tau) = -1$. A physiological example is the measurement of transmission delays (neural or muscular) to determine the conduction velocity of the signal. Consider Figure 2.5, where the signal is stimulated and is recorded at sites S1 and S2; the distance between the sites is d. The time delay between the S1 and S2 is t as determined from $R_{S1S2}(\tau)$, the cross-correlation of S1 and S2. Figure 2.5 shows a peak at $\tau_1 = t$ when S2 is shifted so that it is in phase with S1.

Property #3. The Fourier transform of the cross-correlation function is the cross spectral density function, which is used to calculate the coherence function, which is a measure of the common frequencies present in the two signals. This is a valuable tool in determining the transfer function of a system in which you cannot control the frequency content of the input signal. For example, in determining the transfer function of a muscle with EMG as an input and force an output, we cannot control the input frequencies (Bobet and Norman, 1990).

2.1.5 Importance in Removing the Mean Bias from the Signal

A caution that must be heeded when cross correlating two signals is that the mean (dc bias) in both signals must be removed prior calculating $R_{xy}(\tau)$. Most

standard programs do this without your knowledge, but if you are writing your own program, you must do so or a major error will result. Consider $x(t) = s_1(t) + m_1$ and $y(t) = s_2(t) + m_2$, where m_1 and m_2 are the means of s_1 and s_2, respectively.

$$R_{xy}(\tau) = \int_0^T (s_1(t) + m_1)\,(s_2(t+\tau) + m_2)\,dt$$

$$= \int_0^T s_1(t)s_2(t+\tau)dt + \int_0^T m_1 s_2(t+\tau)dt$$

$$+ \int_0^T m_2 s_1(t)dt + \int_0^T m_1 m_2 dt$$

Since the signals and $m1$ and $m2$ are uncorrelated, the 2nd and 3rd terms will $= 0$.

$$\therefore R_{xy}(\tau) = \int_0^T s_1(t)s_2(t+\tau)dt + \int_0^T m_1 m_2 dt$$

The 1st term is the desired cross-correlation, but a major bias will added by the 2nd term, and the peak of $R_{xy}(\tau)$ may be grossly exaggerated.

2.1.6 Digital Implementation of Auto- and Cross-Correlation Functions

Since data are now routinely collected and stored in a computer, the implementation of the auto- and cross-correlation is the digital equivalent of Equations (2.2) and (2.3), shown below in Equations (2.8) and (2.9)

$$R_{xx}(\tau) = \frac{\frac{1}{N}\sum_{n=1}^{N}[(x(n) - \overline{x})(x(n+\tau) - \overline{x})]}{\frac{1}{N}\sum_{n=1}^{N}(x(n) - \overline{x})^2} \tag{2.8}$$

$$R_{xy}(\tau) = \frac{\frac{1}{N}\sum_{n=1}^{N}\left[(x(n) - \overline{x})(y(n+\tau) - \overline{y})\right]}{\frac{1}{N}\sum_{n=1}^{N}(x(n) - \overline{x})(y(n) - \overline{y})} \tag{2.9}$$

Both auto- and cross-correlations are calculated for various phase shifts that a priori must be specified by the user, and this will have an impact on the number of data points used in the formulae. If, for example, $x(n)$ and $y(n)$ are 1000 data points, and it is desired that $\tau = \pm 100$, then we can only get 800 cross products and, therefore, N will be set to 800. Sometimes the signals of interest are periodic (such as gait); then, we can wrap the signal on itself and calculate the correlations using all the data points. Such an analysis is known as a circular correlation.

2.1.7 Application of Autocorrelations

As indicated in property #3 an autocorrelation indicates the frequency content of $x(t)$. Figure 2.6 presents an EMG record and its autocorrelation. The upper trace (a) is the raw EMG signal, which does not show any visible evidence of hum, but the autocorrelation seen in the lower trace (b) is an even function as predicted by property #2 and shows the presence of 60 Hz hum. Note from Figure 2.3 that $R_{xx}(\tau)$ for a sinusoidal wave has its first zero crossing at $^1/_4$ of a cycle of the sinusoidal frequency; thus, we can use that first zero crossing of $R_{xx}(\tau)$ to estimate the average frequency in the EMG. The first zero crossing for this $R_{xx}(\tau)$ occurred at about 3ms, representing an average period of 12 ms, or an average frequency of about 83 Hz.

2.1.8 Applications of Cross-Correlations

2.1.8.1 Quantification of Cross-Talk in Surface Electromyography. Cross-correlations quantify what is in common in the profiles of $x(t)$ and $y(t)$ but also any common signal present in both $x(t)$ and $y(t)$. This may be true in the recordings from surface electrodes that are close enough to be subject to cross-talk. Because a knowledge of surface recording techniques and the biophysical basis of the EMG signal is necessary to understand cross-talk, the student is referred to Section 10.2.5 in Chapter 10 for a detailed description of how $R_{xy}(\tau)$ has been used to quantify cross-talk.

2.1.8.2 Measurement of Delay between Physiological Signals. Experimental research conducted to find the phase advance of one EMG signal ahead of another has been used to advantage to find balance strategies in walking (Prince et al., 1994). Balance of the head and trunk during gait against large inertial forces is achieved by the paraspinal muscles. It was noted that the head anterior/posterior (A/P) accelerations were severely attenuated ($0.48\,m/s^2$) compared with hip accelerations ($1.91\,m/s^2$), and it was important to determine how the activity of the paraspinal muscles contributed to this reduced head acceleration. The EMG profiles at nine vertebral levels from C7 down to L4 were analyzed to find the time delays between those balance muscles. Figure 2.7 presents the ensemble average (see Section 2.3

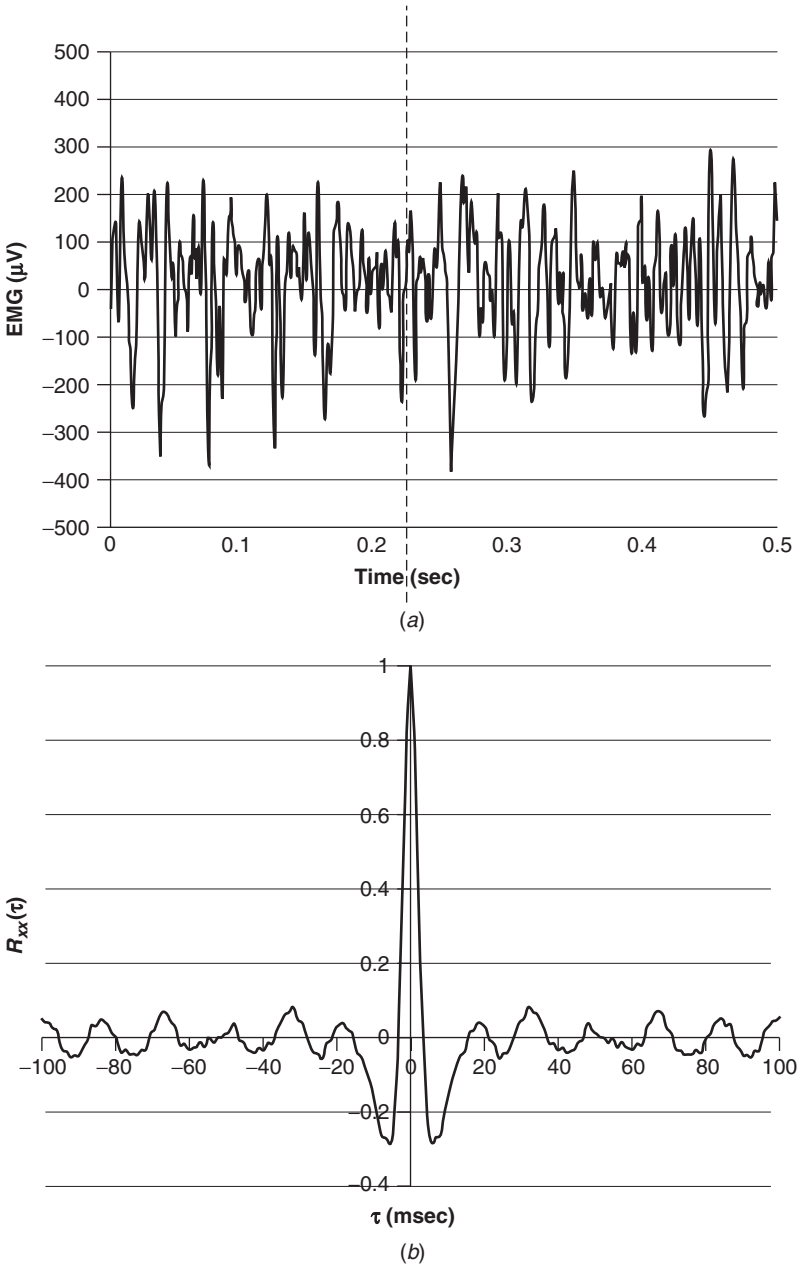

Figure 2.6 *(a)* is a surface EMG signal recorded for 0.5 sec that does not show the presence of any 60 Hz hum pickup. *(b)* is the autocorrelation of this EMG over a $\tau = \pm 100$ ms. Again, note that this is an even function and observe the presence of a periodic component closely resembling a sinusoidal wave with peaks equal to the period of a 60 Hz (approximately 17 ms).

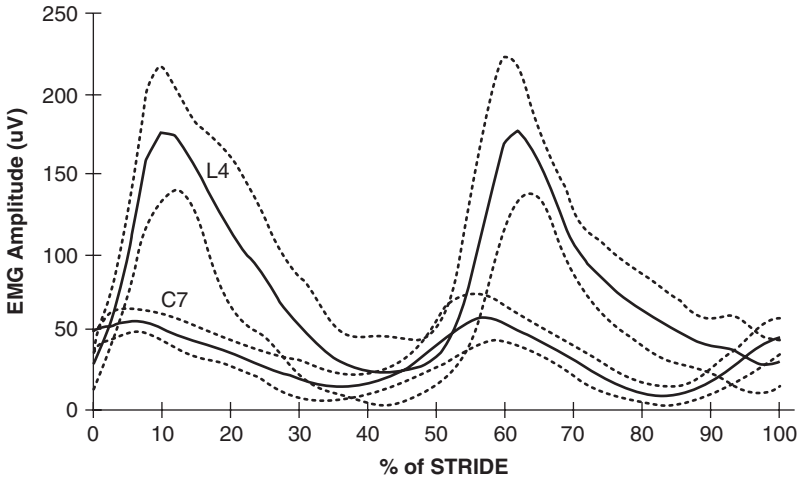

Figure 2.7 Ensemble-averaged profiles over the stride period of EMG signals of paraspinal muscles at C_7 and L_4 levels for one of the subjects. Note the 2nd harmonic peaks occurring during the weight acceptance periods of the left and right feet to balance the trunk and head. The C_7 amplitude is lower than the L_4 amplitude because the inertial load above C_7 is considerably lower than that above L_4. More important is the timing of C_7 so that it is ahead of L_4, indicating that the head is balanced first, ahead of the trunk. (Reproduced by permission from *Gait and Posture*)

later) of L4 and C7 muscle profiles over the stride period for one subject). A cross-correlation of these two signals showed that C7 was in advance of L4 by about 70 ms. For all 10 young adults in this study, all signals at C7, T2, T4, T6, T8, T10, T12, and L2 were separately cross correlated with the L4 profile. The phase shift of these signals is presented in Figure 2.8. The earlier turn on of the more superior paraspinal muscles indicates a "top-down" anticipatory strategy to stabilize the head first, then the cervical level, the thoracic level, and finally the lumbar level. This strategy resulted in a dramatic decrease in the A/P head acceleration over the stride period compared to the A/P acceleration of the pelvis. In a subsequent study on fit and healthy elderly (Wieman, 1991) the head/hip acceleration (%) in the elderly (41.9%) was significantly higher ($p < .02$) compared with that of young adults (22.7%); this indicated that the elderly had lost this "top-down" anticipatory strategy, and the paraspinal EMG profiles bore this out.

2.1.8.3 Measurement of Synergistic and Coactivation EMG Profiles. There is considerable information in EMG profiles regarding the action of agonist/antagonist muscle groups during any given activity. Recently, cross-correlation techniques have been used to quantify coactivation patterns (agonist/antagonist active at the same time) and non-coactivation patterns (agonist/antagonist having synergistic out of phase patterns): Nelson-Wong

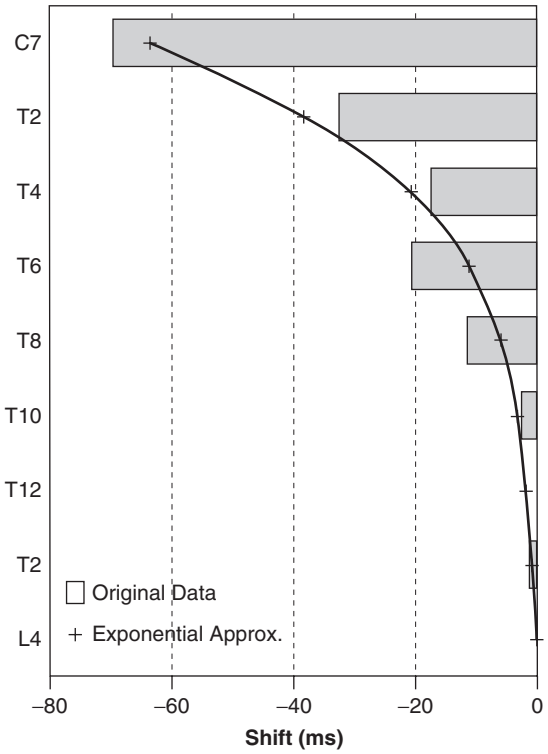

Figure 2.8 Phase shift (ms) of the activation profiles of the paraspinal muscles relative to the profile at the L_4 level. The negative shift indicates the activation was in advance of L_4. The curve fit was exponential. (Reproduced by permission from *Gait and Posture*)

et al. (2008) reported a study of left and right gluteus medius patterns during a long duration standing manual task. Because these patterns are an excellent example of motor synergies and are also related to another medial/lateral postural strategy their details are presented in Chapter 11.

2.2 FREQUENCY ANALYSIS

2.2.1 Introduction—Time Domain vs. Frequency Domain

All the signals that we measure and analyze have a characteristic frequency content, which we refer to as the signal spectrum; this is a plot of all the harmonics in the signal from the lowest to the highest. The purpose of this section is to provide a conceptual background with sufficient mathematical derivations to help the student collect and process data and be an intelligent collector and consumer of commercial software. Frequency domain analysis uses a powerful transform called the Fourier transform, named after Baron

Jean-Baptiste-Joseph Fourier, a French mathematician who developed the technique in 1807.

The knowledge of the frequency spectrum of any given signal is mandatory in making decisions about collection and processing of any given signal. The spectrum decides the sampling rate you must chose before an analog-to-digital conversion is done, and it also decides the length of record that must be converted. Also, the spectrum influences the frequency of filtering of the data to remove undesirable noise and movement artifacts. All these factors will be discussed in the sections to come.

2.2.2 Discrete Fourier (Harmonic) Analysis

1. *Alternating Signals*. An alternating signal (often called ac, for alternating current) is one that continuously changes over time. It may be periodic or completely random, or a combination of both. Also, any signal may have a dc (direct current) component, which may be defined as the bias value about which the ac component fluctuates. Figure 2.9 shows example signals.
2. *Frequency Content*. Any of these signals can also be discussed in terms of their frequency content. A sine (or cosine) waveform is a single frequency; any other waveform can be the sum of a number of sine and cosine waves.

Note that the Fourier transformation (see Figure 2.10) of periodic signals has discrete frequencies, while nonperiodic signals have a continuous spectrum defined by its lowest frequency, f_1, and its highest frequency, f_2. To analyze a periodic signal, we must express the frequency content in multiples

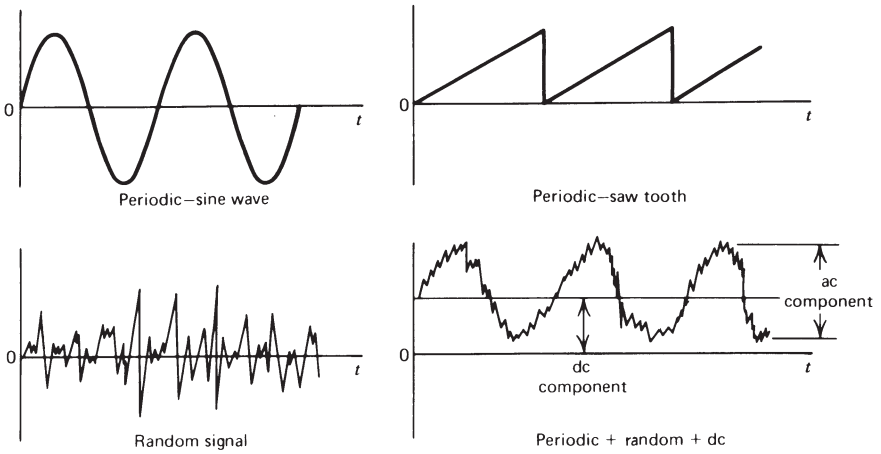

Figure 2.9 Time-related waveforms demonstrate the different types of signals that may be processed.

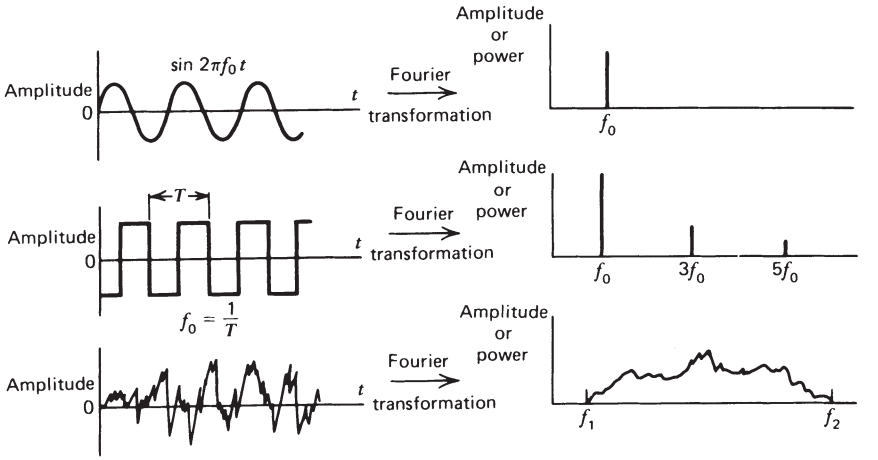

Figure 2.10 Relationship between a signal as seen in the time domain and its equivalent in the frequency domain.

of the fundamental frequency f_0. These higher frequencies are called *harmonics*. The third harmonic is $3f_0$, and the tenth harmonic is $10f_0$. Any perfectly periodic signal can be broken down into its harmonic components. The sum of the proper amplitudes of these harmonics is called a *Fourier series*.

Thus, a given signal $V(t)$ can be expressed as:

$$V(t) = V_{\text{dc}} + V_1 \sin(\omega_0 t + \theta_1) + V_2 \sin(2\omega_0 t + \theta_2) + \cdots + V_n \sin(n\omega_0 t + \theta_n) \tag{2.10}$$

where $\omega_0 = 2\pi f_0$, and θ_n is the phase angle of the nth harmonic.

For example, a square wave of amplitude V can be described by the Fourier series of odd harmonics:

$$V(t) = \frac{4V}{\pi}\left(\sin\omega_0 t + \frac{1}{3}\sin 3\,\omega_0 t + \frac{1}{5}\sin 5\,\omega_0 t + \cdots\right) \tag{2.11}$$

A triangular wave of duration $2t$ and repeating itself every T seconds is:

$$V(t) = \frac{2Vt}{T}\left[\frac{1}{2} + \left(\frac{2}{\pi}\right)^2 \cos\omega_0 t + \left(\frac{2}{3\pi}\right)^2 \cos 3\,\omega_0 t + \cdots\right] \tag{2.12}$$

Several names are given to the graph showing these frequency components: *spectral plots, harmonic plots*, and *spectral density functions*. Each shows the amplitude or power of each frequency component plotted against frequency; the mathematical process to accomplish this is called a *Fourier transformation*

or *harmonic analysis*. Figure 2.10 shows plots of time-domain signals and their equivalents in the frequency domain.

Care must be used when analyzing or interpreting the results of any harmonic analysis. Such analyses assume that each harmonic component is present with a constant amplitude and phase over the total analysis period. Such consistency is evident in Equation (2.10), where amplitude V_n and phase θ_n are assumed constant. However, in real life each harmonic is not constant in either amplitude or phase. A look at the calculation of the Fourier coefficients is needed for any signal $x(t)$. Over the period of time T, using the *discrete Fourier transform*, we calculate n harmonic coefficients.

$$a_n = \frac{2}{T}\int_0^T x(t)\cos n\omega_0 t \; dt \tag{2.13}$$

$$b_n = \frac{2}{T}\int_0^T x(t)\sin n\omega_0 t \; dt \tag{2.14}$$

$$c_n = \sqrt{a_n^2 + b_n^2}$$

$$\theta_n = \tan^{-1}\left(\frac{a_n}{b_n}\right) \tag{2.15}$$

It should be noted that a_n and b_n are calculated *average* values over the period of time T. Thus, the amplitude c_n and the phase θ_n of the nth harmonic are average values as well. A certain harmonic may be present only for part of the time T, but the computer analysis will return an average value, assuming that it is present over the entire time. The fact that a_n and b_n are average values is important when we attempt to reconstitute the original signal as is demonstrated in Section 2.2.4.5.

The digital equivalent of the Fourier transform is important to review because it gives us some insight into the number of calculations that are necessary. In digital form, Equations (2.13) and (2.14) for N samples during the period T:

$$a_n = \frac{2}{N}\sum_{i=0}^{N} x_i \cos(n\omega_0 i/N) \tag{2.16}$$

$$b_n = \frac{2}{N}\sum_{i=0}^{N} x_i \sin(n\omega_0 i/N) \tag{2.17}$$

For each of the n harmonics, N calculations are necessary. The number of harmonics that can be analyzed is from the fundamental ($n = 1$) up to the Nyquist frequency, which is when there are two samples per sine or cosine wave or when $n = N/2$. Therefore, for $N/2$ harmonics, there are $N^2/2$ calculations necessary for each of the sine or cosine coefficients. The total number

of calculations is N^2. It should be noted that the major expense in computer time is looking up the sine and cosine values for each of the N angles.

2.2.3 Fast Fourier Transform (FFT)

The Fast Fourier Transform (FFT) became necessary because of the extremely large number of calculations necessary in the Discrete Fourier Transform. As early as 1942, Danielson and Lanczos introduced the *Danielson-Lanczos Lemma*, which showed that the Discrete Fourier Transform of length N can be broken into two separate odd and even numbered components of length $N/2$ each. In a similar manner, each $N/2$ component can be broken into two more odd and even numbered components of length $N/4$ each, and each of these can be broken into two more odd and even components of length $N/8$ each. Thus, the basis of the FFT is a data record that must be binary in length. Therefore, if you collect data files that are not binary in length, the FFT can only accept the largest binary length file within your data file. For example, if you collected 1000 data points, the largest binary file length would be 512 points; thus, 488 points would be wasted. Therefore, it is advisable to prearrange data collection files to be binary in length; in the case of the previous example, a data file of 1024 points would be appropriate. With the advent of computers, many FFT algorithms appeared (Bringham, 1974), and in the mid-1960s J. W. Cooley and J. W. Tukey at IBM developed what is probably the best-known FFT algorithm.

One of the major savings in the FFT is to avoid repetitive and time-consuming calculations especially sines and cosines. If we look at Equations (2.16) and (2.17), we see that for the fundamental frequency ($n = 1$), we must calculate N sine and N cosine values. For the second harmonic, we recalculate every second sine and cosine value, and for the third harmonic we recalculate every third sine and cosine value, and so on up to the highest harmonic. What the FFT does is calculate all sine and cosine values for the fundamental and this forms a "look-up" table for the fundamental plus all higher harmonics. Further savings are achieved by clustering all the products of x_i and the same sine value, then summing all the x_i values, and then carrying out one product with the sine value. The number of calculations for the FFT $= N \log_2 N$, which is considerably less than N^2 for the Discrete Fourier Transform. For example, for $N = 4096$ and a CPU cycle time of 0.1 μs the DFT would take $4096^2 10^{-7} = 1.67$ s, while the FFT would take $4096 \log_2 4096 \cdot 10^{-7} = 49$ ms.

2.2.4 Applications of Spectrum Analyses

2.2.4.1 Analog-to-Digital Converters. To students not familiar with electronics, the process that takes place during conversion of a physiological signal into a digital computer can be somewhat mystifying. A short schematic description of that process is now given. An electrical signal representing a

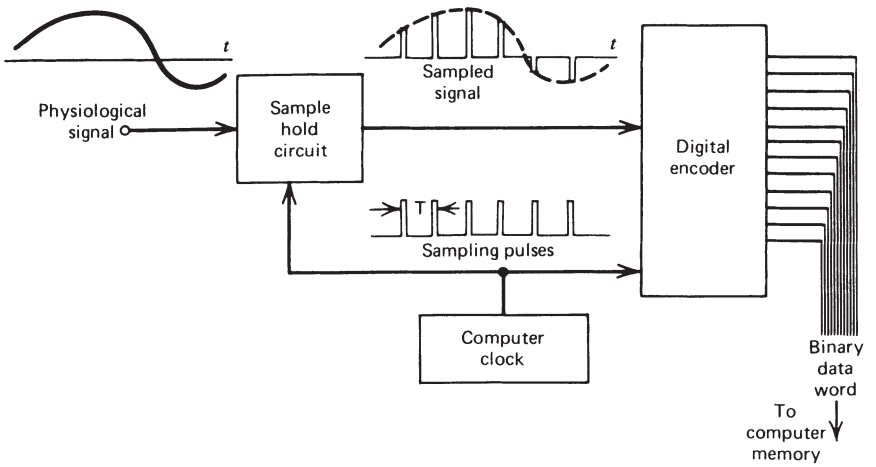

Figure 2.11 Schematic diagram showing the steps involved in an analog-to-digital conversion of a physiological signal.

force, an acceleration, an electromyographic (EMG) potential, or the like is fed into the input terminals of the analog-to-digital converter. The computer controls the rate at which the signal is sampled; the optimal rate is governed by the sampling theorem (see Section 2.2.4.2).

Figure 2.11 depicts the various stages in the conversion process. The first is a sample/hold circuit in which the analog input signal is changed into a series of short-duration pulses, each one equal in amplitude to the original analog signal at the time of sampling. The final stage of conversion is to translate the amplitude and polarity of the sampled pulse into digital format. This is usually a binary code in which the signal is represented by a number of bits. For example, a 12-bit code represents $2^{12} = 4096$ levels. This means that the original sampled analog signal can be broken into 4096 discrete amplitude levels with a unique code representing each of these levels. Each coded sample (consisting of 0s and 1s) forms a 12-bit "word," which is rapidly stored in computer memory for recall at a later time. If a 5-s signal were converted at a sampling rate of 100 times per second, there would be 500 data words stored in memory to represent the original 5-s signal.

2.2.4.2 Deciding the Sampling Rate—The Sampling Theorem. In the processing of any time-varying data, no matter what their source, the sampling theorem must not be violated. Without going into the mathematics of the sampling process, the theorem states that "the process signal must be sampled at a frequency at least twice as high as the highest frequency present in the signal itself." If we sample a signal at too low a frequency, we get aliasing errors. This results in false frequencies, frequencies that were not present in the original signal, being generated in the sample data. Figure 2.12 illustrates

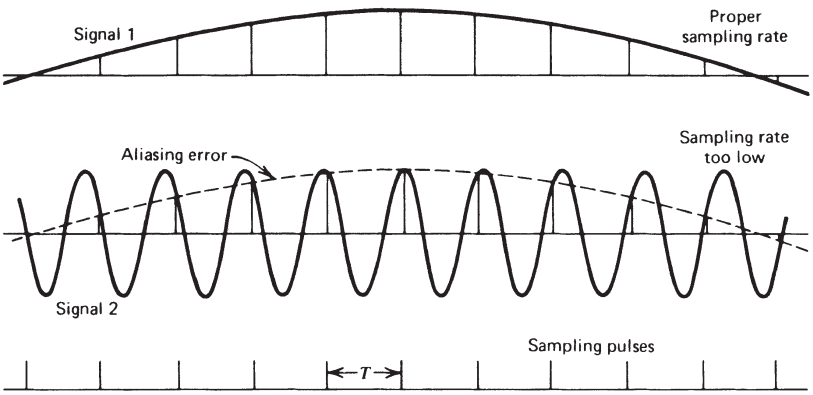

Figure 2.12 Sampling of two signals, one at a proper rate, the other at too low a rate. Signal 2 is sampled at a rate less than twice its frequency, such that its sampled amplitudes are the same as for signal 1. This represents a violation of the sampling theorem and results in an error called *aliasing*.

this effect. Both signals are being sampled at the same interval T. Signal 1 is being sampled about 10 times per cycle, while signal 2 is being sampled less than twice per cycle. Note that the amplitudes of the samples taken from signal 2 are identical to those sampled from signal 1. A false set of sampled data has been generated from signal 2 because the sample rate is too low—the sampling theorem has been violated.

The tendency of those using film is to play it safe and film at too high a rate. Usually, there is a cost associated with such a decision. The initial cost is probably in the equipment required. A high-speed movie camera can cost four or five times as much as a standard model (24 frames per second). Or a special optoelectric system complete with the necessary computer can be a $70,000 decision. In addition to these capital costs, there are the higher operational costs of converting the data and running the necessary kinematic and kinetic computer programs. Except for high-speed running and athletic movements, it is quite adequate to use a standard movie or television camera. For normal and pathological gait studies, it has been shown that kinetic and energy analyses can be done with negligible error using a standard 24–frame per second movie camera (Winter, 1982). Figure 2.13 compares the results of kinematic analysis of the foot during normal walking, where a 50-Hz film rate was compared with 25 Hz. The data were collected at 50 Hz, and the acceleration of the foot was calculated using every frame of data, then reanalyzed again, using every second frame of converted data. It can be seen that the difference between the curves is minimal; only at the peak negative acceleration was there a noticeable difference. The final decision as to whether this error is acceptable should not rest in this curve, but in your final goal. If, for example, the final analysis was a hip and knee torque analysis, the acceleration of the foot segment may not be too important, as is evident from

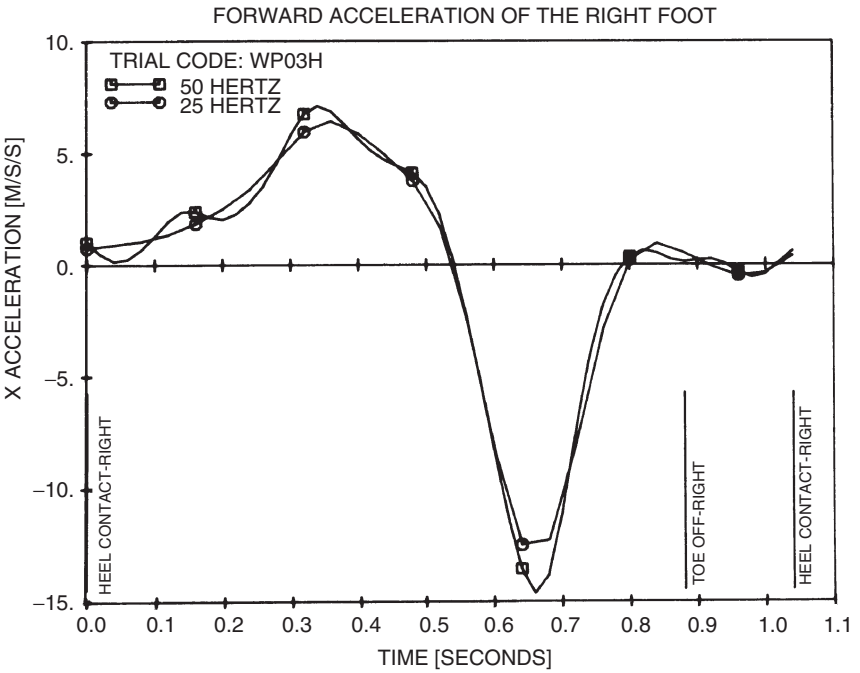

Figure 2.13 Comparison of the forward acceleration of the right foot during walking using the same data sampled at 50 Hz and at 25 Hz (using data from every second frame). The major pattern is maintained with minor errors at the peaks.

another walking trial, shown in Figure 2.14. The minor differences in no way interfere with the general pattern of joint torques over the stride period, and the assessment of the motor patterns would be identical. Thus, for movements such as walking or for slow movements, an inexpensive camera at 24 frames per second appears to be quite adequate.

2.2.4.3 Deciding the Record Length. The duration of record length is decided by the lowest frequency present in the signal. In cyclical events such as walking, cycling, or swimming the lowest frequency is easy to determine; it is the stride frequency or how often each segment of the body repeats itself. For example, if a patient is walking at 105 steps/min the step frequency is $105/60 = 1.75$ steps/s $= 0.875$ strides/s. Thus, the fundamental frequency is 0.875 Hz. However, there are a number of noncyclical movements, which do not have a defined lowest frequency. One such "movement" is standing either quietly or in a work-related task. In quiet standing, we model the total body as an inverted pendulum (Gage et al., 2004), which simplifies the total body into a single weighted-average center of mass (COM) and which can be compared with the center of pressure (COP) measured from the force plate. Figure 2.15 presents a typical FFT of the COP and COM in the anterior/posterior direction

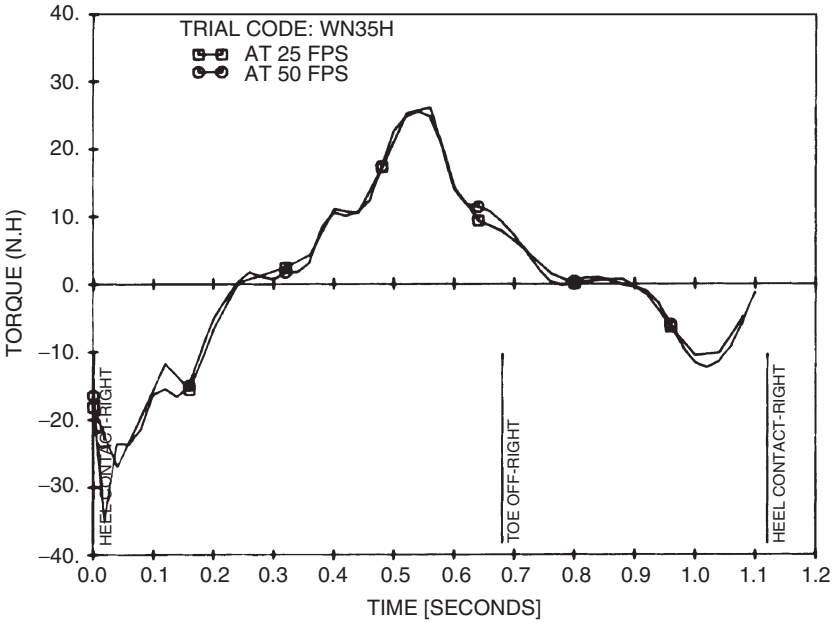

Figure 2.14 Comparison of the hip moment of force during level walking using the same data sampled at 50 Hz and at 25 Hz. The residual error is quite small because the joint reaction forces dominate the inertial contributions to the net moment of force.

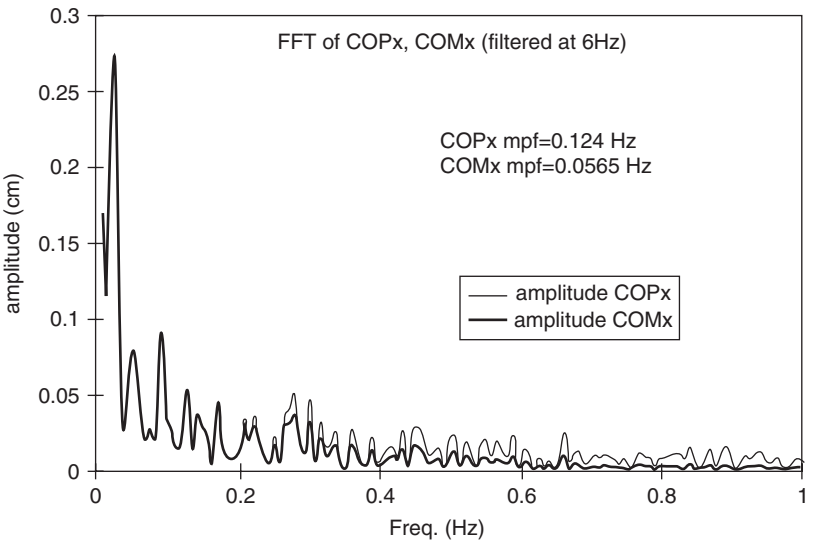

Figure 2.15 FFT of the COM and COP in the anterior/posterior direction of a subject standing quietly for 137 seconds. (Winter, D. A., A.B.C. *(Anatomy, Biomechanics, and Control) of Balance During Standing and Walking*. Waterloo Biomechanics. 1995)

for a subject standing quietly for 137 seconds (8192 samples @ 60 Hz). Note that the FFT plots the amplitude of each harmonic from 0.0073 Hz to 1 Hz. Also note the dominant low frequency components of both COM and COP below 0.2 Hz. The length of record must be at least a minute or longer. This long record may be compromised when studying patients with balance disorders because they may not be able to stand quietly for that length of time. However, for studies on normal subjects Carpenter, et al. (2001) found that records of at least one minute were required for acceptable reliability.

2.2.4.4 Analog and Digital Filtering of Signals—Noise and Movement Artifacts. The basic approach can be described by analyzing the frequency spectrum of both signal and noise. Figure 2.16*a* shows a schematic plot of a signal and noise spectrum. As can be seen, the signal is assumed to occupy the lower end of the frequency spectrum and overlaps with the noise, which is usually higher frequency. Filtering of any signal is aimed at the selective rejection, or attenuation, of certain frequencies. In the preceding case, the obvious filter is one that passes, unattenuated, the lower-frequency signals, while at the same time attenuating the higher-frequency noise. Such a filter, called a *low-pass filter*, has a frequency response as shown in Figure 2.16*b*. The frequency response of the filter is the ratio of the output $X_o(f)$ of the filter to its input $X_i(f)$ at each frequency present. As can be seen, the response at lower frequencies is 1.0. This means that the input signal passes through the filter unattenuated. However, there is a sharp transition at the cutoff frequency f_c so that the signals above f_c are severely attenuated. The net result of the filtering process can be seen by plotting the spectrum of the output signal $X_o(f)$ as seen in Figure 2.16*c*. Two things should be noted. First, the higher-frequency noise has been severely reduced but not completely rejected. Second, the signal, especially in the region where the signal and noise overlap (usually around f_c) is also slightly attenuated. This results in a slight distortion of the signal. Thus, a compromise has to be made in the selection of the cutoff frequency. If f_c is set too high, less signal distortion occurs, but too much noise is allowed to pass. Conversely, if f_c is too low, the noise is reduced drastically, but at the expense of increased signal distortion. A sharper cutoff filter will improve matters, but at an additional expense. In digital filtering, this means a more complex digital filter and, thus, more computer time.

The first aspect that must be assessed is what the signal spectrum is as opposed to the noise spectrum. This can readily be done, as is seen in the harmonic analysis for 20 subjects presented in Figure 2.17. Here is the harmonic content of the vertical displacement of the toe marker in natural walking (Winter et al., 1974). The highest harmonics were found to be in the toe and heel trajectories, and it was found that 99.7% of the signal power was contained in the lower seven harmonics (below 6 Hz). Above the seventh harmonic, there was still some signal power, but it had the characteristics of "noise." Noise is the term used to describe components of the final signal

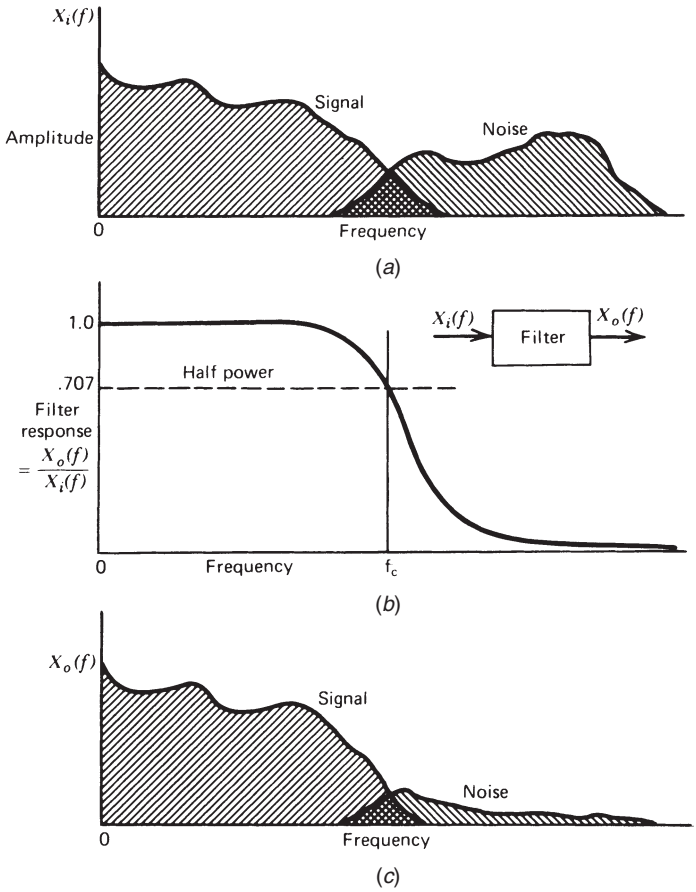

Figure 2.16 (*a*) Hypothetical frequency spectrum of a waveform consisting of a desired signal and unwanted higher-frequency noise. (*b*) Response of low-pass filter $X_o(f)/X_i(f)$, introduced to attenuate the noise. (*c*) Spectrum of the output waveform, obtained by multiplying the amplitude of the input by the filter response at each frequency. Higher-frequency noise is severely attenuated, while the signal is passed with only minor distortion in transition region around f_c.

that are not the result of the process itself (in this case, walking). Noise comes from many sources: electronic noise in optoelectric devices, spatial precision of the TV scan or film digitizing system, and human error in film digitizing. If the total effect of all these errors is random, then the true signal will have an added random component. Usually, the random component is high frequency, as is borne out in Figure 2.17. Here, we see evidence of higher-frequency components extending up to the 20th harmonic, which was the highest frequency analyzed. The presence of the higher-frequency noise is of considerable importance when we consider the problem of trying to

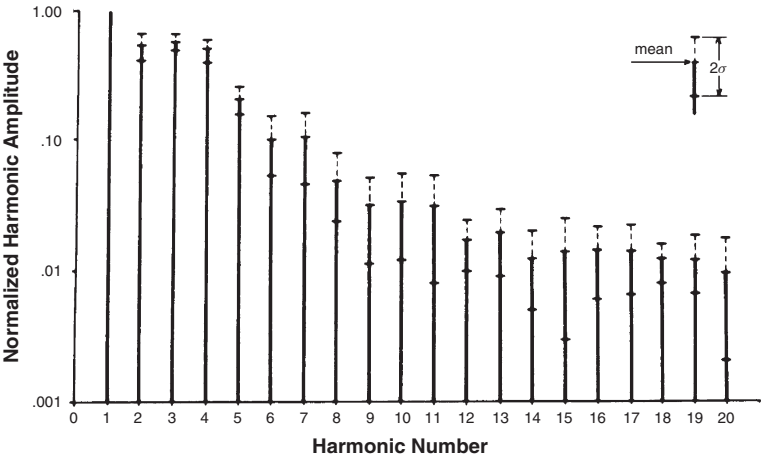

Figure 2.17 Harmonic content of the vertical displacement of a toe marker from 20 subjects during normal walking. Fundamental frequency (harmonic number = 1) is normalized at 1.00. Over 99% of power is contained below the seventh harmonic. (Reproduced by permission from the *Journal of Biomechanics*.)

calculate velocities and accelerations from the displacement data, as will be evident later in Section 3.4.3.

The theory behind digital filtering (Radar and Gold, 1967) will not be covered, but the application of low-pass digital filtering will be described in detail. As a result of the previous discussion for these data on walking, the cutoff frequency of a digital filter should be set at about 6 Hz. The format of a recursive digital filter that processes the raw data in time domain is as follows:

$$X^1(nT) = a_0X(nT) + a_1X(nT - T) + a_2X(nT - 2T) + b_1X^1(nT - T) + b_2X^1(nT - 2T) \quad (2.18)$$

where X^1 = filtered output coordinates
X = unfiltered coordinate data
nT = nth sample
$(nT - T)$ = $(n-1)$th sample
$(nT - 2T)$ = $(n-2)$th sample
$a_0, \ldots, b_0, \ldots$ = filter coefficients

These filter coefficients a_0, a_1, a_2, b_1 and b_2 are constants that depend on the type and order of the filter, the sampling frequency, and the cutoff frequency. As can be seen, the filter output $X^1(nT)$ is a weighted version of the immediate and past raw data plus a weighted contribution of past filtered output. The

exact equations to calculate the coefficients for a Butterworth or a critically damped filter are as follows:

$$\omega_c = \frac{(\tan(\pi f_c / f_s))}{C} \tag{2.19}$$

where C is the correction factor for number of passes required, to be explained shortly. For a single pass filter $C = 1$.

$K = \sqrt{2}\omega_c$ for a Butterworth filter,

or, 2 ω_c for a critically damped filter

$$K_2 = \omega_c^2, \quad a_0 = \frac{K_2}{(1 + K_1 + K_2)}, \quad a_1 = 2a_0, \quad a_2 = a_0$$

$$K_3 = \frac{2a_0}{K_2}, \quad b_1 = -2a_0 + K_3$$

$$b_2 = 1 - 2a_0 - K_3, \qquad \text{or} \qquad b_2 = 1 - a_0 - a_1 - a_2 - b_1$$

For example, a Butterworth-type low-pass filter of second order is to be designed to cutoff at 6 Hz using film data taken at 60 Hz (60 frames per second). As seen in Equation (2.19) the only thing that is required to determine these coefficients is the ratio of sampling frequency to cutoff frequency. In this case it is 10. The design of such a filter would yield the following coefficients:

$$a_0 = 0.067455, \quad a_1 = 0.13491, \quad a_2 = 0.067455,$$
$$b_1 = 1.14298, \quad b_2 = -0.41280$$

Note that the algebraic sum of all the coefficients equals 1.0000. This gives a response of unity over the passband. Note that the same filter coefficients could be used in many different applications, as long as the ratio f_s/f_c is the same. For example, an EMG signal sampled at 2000 Hz with cutoff desired at 400 Hz would have the same coefficients as one employed for movie film coordinates where the film rate was 30 Hz and cutoff was 6 Hz. The number of passes, C, in Equation (2.17) are important when filtering kinematic data in order to eliminate the phase shift of the filtered data. This aspect of digital filtering of kinematic data will be detailed later in Section 3.4.4.2.

2.2.4.5 Fourier Reconstitution of Original Signal. Figure 2.18 is presented to illustrate a Fourier reconstitution of the vertical trajectory of the heel of an adult walking his or her natural cadence. A total of nine harmonics is represented here because the addition of higher harmonics did not improve the curve of the original data. As can be seen, the harmonic reconstitution is visibly different from the original, sufficiently so as to cause reasonable

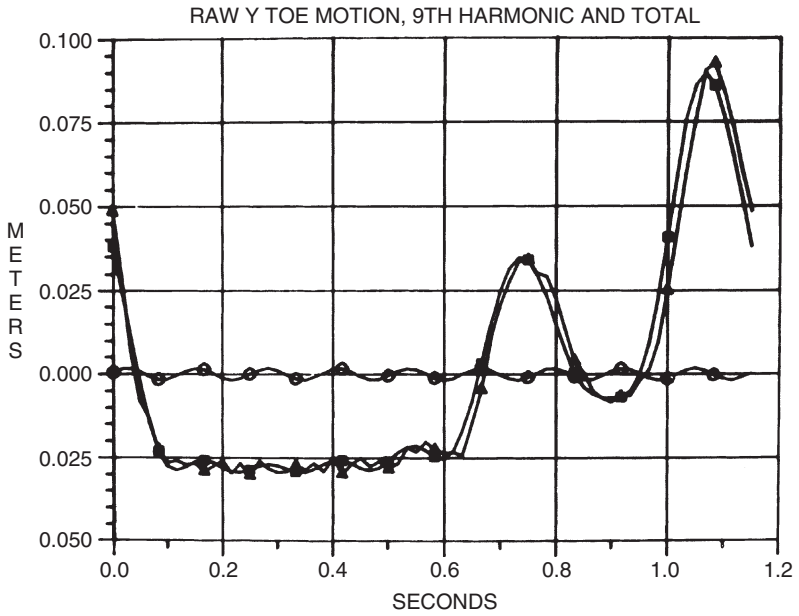

Figure 2.18 Fourier reconstruction of the vertical trajectory of a toe marker during one walking stride. The actual trajectory is shown by the open square, the reconstruction from the first nine harmonics is plotted with open triangles, and the contribution of the ninth harmonic is plotted with open circles. The difference between the actual and the reconstructed waveforms is the result of the lack of stationarity in the original signal.

errors in subsequent biomechanical analyses. This is because each harmonic amplitude and phase values are average values, as we cautioned about in Section 2.22, and this is especially true for a foot marker during gait, which has high frequencies during swing and low frequencies during stance.

2.2.4.6 Fourier Analysis of White Noise. White noise was introduced in Figure 2.4, where an autocorrelation showed that each point has zero correlation with any points ahead or behind it in time. In a computer, white noise can be simulated by a random number generator. The other characteristic of white noise is in the frequency domain where the frequency spectrum is equal across the whole range of the signal, and this is similar to some of the noise apparent in kinematic data—cine, television, and optoelectric systems. To demonstrate this frequency spectum characteristic we present an analysis of the FFT of white noise. Figure 2.19 (a) is a white noise signal simulated on Excel from a random number generator with amplitude ± 1 sampled at a rate of 2048 samples/sec. Thus, the highest frequency present in this signal is the Nyquist frequency of 1024 Hz, so our FFT will cover frequencies from 0 Hz to 1024 Hz. An FFT of the signal in Figure 2.19 (a) is presented in Figure 2.19 (b). Note that the spectrum over that range appears "noisy," but

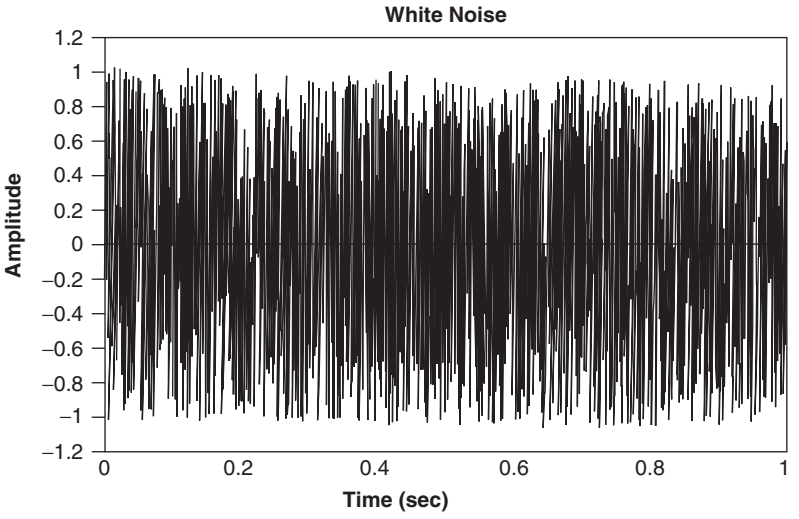

(*a*)

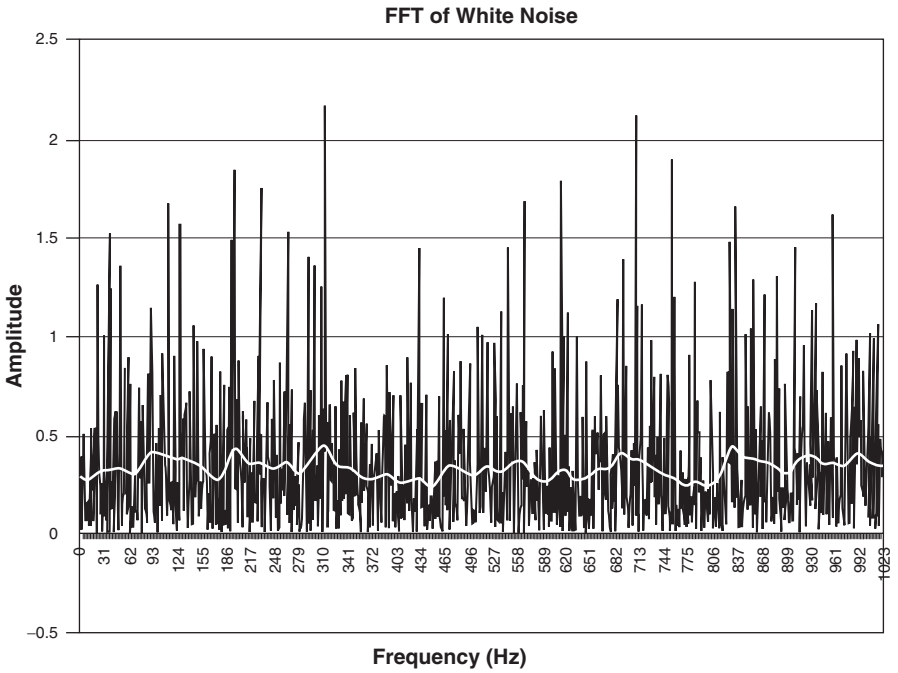

(*b*)

Figure 2.19 *(a)* A simulated white noise signal from a random number generator with amplitude ± 1 samples at 2048 samples/sec. Figure 2.19 *(b)* is the FFT of the white noise signal at 1 Hz intervals from 0 Hz to 1024 Hz. The "white" line passing through this FFT plot is a 40-point moving average showing that the signal has approximately equal power across the full spectrum of the signal.

that is because of the fact that the FFT is plotting the amplitude at every single Hz. A more realistic plot of this spectrum is to carry out a moving average across the full spectrum, and this was done with a 40-point moving average, which is the "white" curve in Figure 2.19 (b). This moving average approaches the theoretical constant amplitude across the full spectrum; its average amplitude is 0.330 and ranges from 0.233 to 0.446. A longer time domain record than the 2048 points will result in a more constant frequency plot. Also, it should be noted that some of the individual harmonic amplitudes are greater than one, and this is not expected from the white noise signal, which had an amplitude of ± 1. What is not shown here are the phase angles of each of the harmonics; each has a different phase angle, so there will be many cancellations as each harmonic is added.

2.3 ENSEMBLE AVERAGING OF REPETITIVE WAVEFORMS

A large number of movements that we study are cyclical in nature and, therefore, can benefit from a cyclical average of its many variables. Gait (walking and running) is the most common repetitive movement but cycling, rowing, and lifting also benefit from such averaged profiles. Both intra- and inter-subject averaged profile have been reported on a wide variety of kinematic, kinetic and EMG variables. The major benefit of such a technique is that the averaged waveform is more reliable and the variation about the mean gives us additional information as to the randomness of the variable. For example, in gait the intra-subject lower limb joint angles have minimal variability, while the moment profiles at these same joints are quite variable. This phenomenon has resulted in a covariance analysis, which can readily be done; we can calculate the mean variance at each of the joints from these ensemble averages, from which the covariances can be determined. As a result of those analyses, a total lower limb motor synergy has been identified, and this is reported in detail in Chapter 11. Such ensemble-averaged waveforms also form the basis of clinical assessments, where the patient's profile superimposed on the average for a comparable healthy group provides a very powerful tool in diagnosing specific motor abnormalities. An example of such a clinical analysis is presented in the next section, Section 2.3.1.

2.3.1 Examples of Ensemble-Averaged Profiles

Figure 2.20 shows a typical waveform from a clinical gait study of an above-knee amputee; the ankle, knee, and hip moments of the amputee (dashed lines) are overlaid on the averaged profiles for 29 young adults (Winter, 1995). The detailed diagnostics will not be discussed here except to comment that the deviations from normal of each joint moment are readily evident, and these differences may lead to altered therapy or adjustments in the prosthesis. Note the averaged profiles are solid lines with dotted

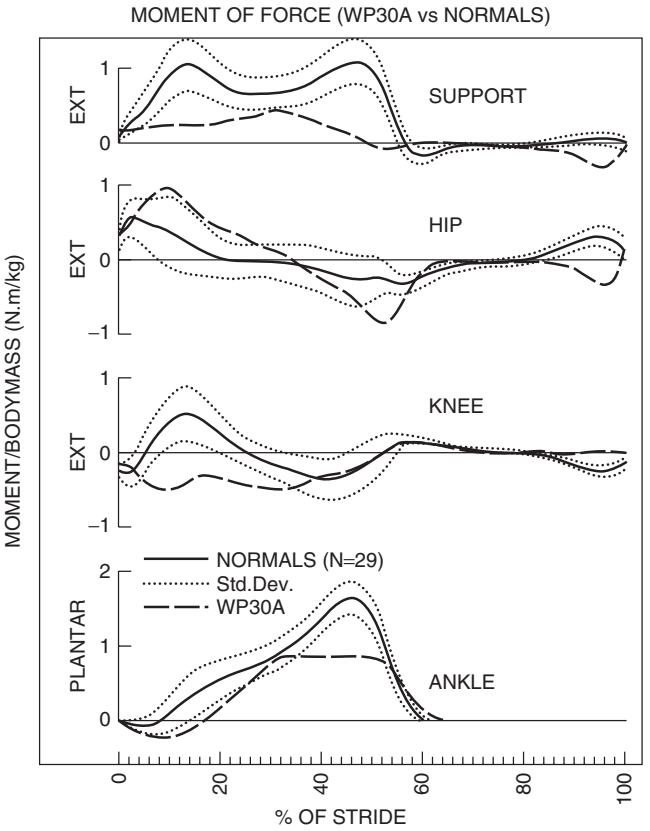

Figure 2.20 Moment-of-force profiles of an above-knee amputee (dashed lines) overlaid on the ensemble-averaged profiles for 29 young adults. The averaged profiles are solid lines with dotted lines representing ± one standard deviation. To reduce the variability of these intersubject moment curves, the joint moments were divided by body mass prior to averaging. (Reproduced with permission from Winter, D.A. *Biomechanics and Motor Control of Human Gait: Normal, Elderly and Pathological, 2nd Ed*. Waterloo Biomechanics, 1995.)

lines representing ± one standard deviation. The units of these intersubject moment-of-force curves are N.m/kg; dividing by body mass was necessary to decrease the variability by about 50%. Also noted is that the cyclical period of one stride has been normalized to 100%. Thus, the process to create these averaged waveforms requires the time base of each subject's profiles to be altered from their individual stride time (in sec) to a 100% stride baseline.

2.3.2 Normalization of Time Bases to 100%

Assume that for one subject there are n samples of a given variable x over the stride period and we wish to normalize this time-domain record to N

samples over the 100% stride period; we will call this normalized curve y. Therefore, each interval of the normalized curve would be n/N samples in duration. Assume that $n = 107$ samples and $N = 100$. At $N = 1$, we need the value of the variable at the 1.07^{th} sample; thus, by linear interpolation, $y_1 = 0.93x_1 + 0.07x_2$; for $N = 2$ we need the value at the 2.14^{th} sample, or $y_2 = 0.86x_2 + 0.14x_;$ for $N = 3$ we need the value at the 3.21^{th} sample, or $y_3 = 0.79x_3 + 0.21x_4$, and so on; for $N = 99$ we need the value at the 105.93^{th} sample, or $y_{99} = 0.07x_{105} + 0.93x_{106;}$ and finally $y_{100} = x_{107}$.

2.3.3 Measure of Average Variability about the Mean Waveform

The most common descriptive statistical measure of data where a single measure is taken is the coefficient of variation, $CV = \sigma/\overline{X}$, where σ is the standard deviation and $\overline{X}$ is the sample mean. The CV is a variability to mean ratio, and with the ensemble average, we wish to calculate a similar variability score; this score is the average σ over the stride period of N points divided by the average signal (absolute value). Some researchers suggest that the rms value of the signal replace the absolute value in the denominator, but this changes the CV scores very little.

$$CV = \frac{\sqrt{\dfrac{1}{N}\displaystyle\sum_{i=1}^{N}\sigma_i^2}}{\dfrac{1}{N}\displaystyle\sum_{i=1}^{N}|X_i|} \tag{2.20}$$

2.4 REFERENCES

Bobet, J. and R. W. Norman. “Least Squares Identification of the Dynamic Relation between the Electromyogram and Joint Moment.’’ *J. Biomech.* **23**: 1275–1276, 1990.

Brigham, E.O. *The Fast Fourier Transform*. (Prentice-Hall, Englewood Cliffs, N.J., 1974).

Carpenter, M. G., J. S. Frank, D. A. Winter, and G. W. Paysar. “Sampling Duration Effects on Centre of Pressure Summary Measures,’’ *Gait and Posture* **13**:35–40, 2001.

Gage, W. G., D. A. Winter, and J. S. Frank. “Kinematic and Kinetic Validation of Inverted Pendulum Model in Quiet Standing,’’ *Gait and Posture* **19**: 124– 132, 2004.

Nelson-Wong, E., D. E. Gregory, D. A. Winter, and J. P. Callaghan. “Gluteus Medius Muscle Activation Patterns as a Predictor of Low Back Pain during Standing,’’ *Clinical Biomechanics* **23**:545–553, 2008.

Prince, F., D. A. Winter, P. Stergiou, and S. E. Walt. "Anticipatory Control of Upper Body Balance during Human Locomotion,'' *Gait and Posture* **2**: 19–25, 1994.

Radar, C. M. and B. Gold. "Digital Filtering Design Techniques in the Frequency Domain,'' *Proc. IEEE* **55**: 149–171, 1967.

Wieman, C. "EMG of the Trunk and Lower Limb Muscles during Gait of Elderly and Younger Subjects: Implications for the Control of Balance.'' MSc Thesis, University of Waterloo, 1991.

Winter, D. A. "Camera Speeds for Normal and Pathological Gait Analysis,'' *Med. Biol. Eng. Comput.* **20**: 408–412, 1982.

Winter, D. A. *The Biomechanics and Motor Control of Human Gait: Normal, Elderly and Pathological*, *2nd Ed.* (Waterloo Biomechanics, Waterloo, Ont. 1995).

Winter, D.A., H.G. Sidwall, and D. A. Hobson. "Measurement and Reduction of Noise in Kinematics of Locomotion,'' *J. Biomech.* **7**: 157–159, 1974.